

# Magnetic resonance imaging for simultaneous morphological and functional evaluation of esophageal motility disorders

Yasuhiro Miyazaki · Kiyokazu Nakajima · Mitsuhiro Sumikawa · Makoto Yamasaki · Tsuyoshi Takahashi · Hiroshi Miyata · Shuji Takiguchi · Yukinori Kurokawa · Noriyuki Tomiyama · Masaki Mori · Yuichiro Doki

Received: 4 January 2013 / Accepted: 25 February 2013 / Published online: 21 May 2013  
© Springer Japan 2013

## Abstract

**Purposes** The purpose of this study was to evaluate the feasibility and safety of esophageal functional magnetic resonance imaging (fMRI) for the diagnosis of achalasia.

**Methods** Eleven patients with suspected achalasia and three normal subjects underwent fMRI while swallowing clear liquid with original sequences; “T2-weighted single-shot fast spin-echo” and “Fast Imaging Employing Steady-state Acquisition”. The fMRI-based diagnosis was compared with that based on manometry. The luminal fluctuation index (LFI) and Dd/Ds ratio were used for the objective evaluation of the esophageal peristalsis and relaxation of the lower esophageal sphincter (LES).

**Results** Functional MRI showed a dilated tortuous esophagus with no tumor, poor clearance, simultaneous waves, aperistalsis, and impaired LES relaxation in all but one case, allowing the diagnosis of achalasia with accuracy similar to that of manometry. The LFI (median 0.08, range 0.03–0.25) and Dd/Ds ratio (1.40, 1.0–2.3) of the patient group were significantly lower than those of the normal subjects [1.50, 2.32–4.05, and 2.59 (2.32–4.05)]. No severe adverse events directly related to fMRI were noted.

**Conclusions** Using our protocol, fMRI was considered to be safe and feasible for the diagnosis of achalasia. Given the widespread use of MRI, esophageal fMRI, which does not require exposure to radiation, could be a potentially useful diagnostic tool for patients with esophageal motility disorders.

**Keywords** Esophagography · Esophagogastroduodenoscopy · Manometry · Achalasia · Magnetic resonance imaging

## Introduction

Achalasia is an idiopathic primary esophageal motility disorder characterized by esophageal aperistalsis and impaired swallow-induced relaxation of the lower esophageal sphincter (LES). It is a rare disease that affects both genders with a prevalence rate of <1/100,000 per year [1–4]. In addition to the typical symptom of dysphagia for both liquids and solids, patients often present with back pain, chest pain, and/or regurgitation. Although these symptoms provide a hint to the diagnosis of achalasia, it is not unusual for it to take a long time to diagnose this condition due to the lack of specific symptoms or abnormal findings on physical examinations [5, 6]. There have been reports of patients with achalasia and prolonged postprandial reflux who have been treated with an acid secretory inhibitor for long periods under the misdiagnosis of gastroesophageal reflux disease (GERD) [7]. Care must be taken to avoid a misdiagnosis of various diseases mimicking achalasia, including cases with esophageal cancer, known as “pseudoachalasia”.

The investigative work-up for dysphagia includes esophagography, esophagogastroduodenoscopy (EGD), and chest/abdominal computed tomography (CT). These modalities are often repeated before sending patients to a

Y. Miyazaki · K. Nakajima (✉) · M. Yamasaki · T. Takahashi · H. Miyata · S. Takiguchi · Y. Kurokawa · M. Mori · Y. Doki

Division of Gastroenterological Surgery, Department of Surgery, Graduate School of Medicine, Osaka University, 2-2 E-2 Yamadaoka, Suita, Osaka 565-0871, Japan  
e-mail: knakajima@gesurg.med.osaka-u.ac.jp

Y. Miyazaki  
e-mail: ymiyazaki02@gesurg.med.osaka-u.ac.jp

M. Sumikawa · N. Tomiyama  
Department of Radiology, Graduate School of Medicine, Osaka University, 2-2 E-2 Yamadaoka, Suita, Osaka 565-0871, Japan

physiological laboratory for esophageal manometry, resulting in a long morbidity period prior to active treatment. A single diagnostic procedure that can evaluate the esophageal morphology and function in one setting may provide an earlier diagnosis, thus benefiting patients by avoiding a prolonged inflammation period. Reducing the pretreatment period may lead to more successful surgery with fewer complications, lower healthcare expenses, and thus, a better overall improvement of the outcome.

Functional magnetic resonance imaging (fMRI) has been widely applied for the diagnosis of a variety of diseases following advances in the development of fast imaging techniques and improved resolution. Although fMRI is currently used in the clinical setting for the evaluation of cardiac and/or macrovascular diseases [8], several reports have advocated using MRI for the functional testing of the esophagus [9–11]. However, the imaging methods described in the literature have varied widely and are all used different types of contrast media. Presently, fMRI is not established as a diagnostic modality for esophageal motility disorders. In addition, there are no objective criteria for the diagnosis of achalasia with fMRI.

We hypothesized that optimization of the imaging sequences would enhance the use of esophageal fMRI without contrast medium, as an investigative modality for achalasia. To test this hypothesis, we evaluated the feasibility, safety, and potential effectiveness of esophageal fMRI with optimized imaging sequences. Based on the findings of the study, we propose new numerical indices for the objective evaluation of esophageal motility using fMRI.

## Materials and methods

### Patients

From April 2010 to October 2011, 11 consecutive patients (four males, seven females, median age 40, range 27–77 years) were referred to our hospital with esophageal obstructive symptoms, e.g., progressive dysphagia, reflux of undigested food and retrosternal chest pain. All patients underwent an initial workup using esophagography, EGD and chest/abdominal CT. In addition, these patients underwent esophageal fMRI according to the imaging protocols described below. A definite diagnosis was made by esophageal manometry. Patients with a confirmed diagnosis of achalasia underwent a laparoscopic Heller-Dor operation. The remaining patients received appropriate treatment depending on the final diagnosis.

### Imaging protocols

All patients fasted overnight to empty the esophagus and reduce the risk of aspiration. Two imaging protocols were

used on a 3.0 T MRI unit (Signa, General Electric, Milwaukee, WI):

### *SSFSE to fixed-slice angles*

Axial T2-weighted single-shot fast spin-echo (SSFSE) MR imaging (TR 1000 ms, TE 80 ms, Bandwidth 62.5, Frequency 288, Phase 160, FOV 35.0 cm, Slice thickness 8 mm, Spacing 1 mm, Asset sense factor 2) was performed from the level of the sternal notch to the upper abdomen, to determine the optimum slice angles for the esophageal body where the longest sagittal slice was required, and the LES, where esophageal motility could be evaluated in a reproducible fashion. In patients with a severely tortuous esophagus, more than two slice angles at one location and oblique images at the esophageal body were necessary to provide an adequate evaluation of the motility.

### *FIESTA for fMRI*

First, one series of dynamic acquisitions for 40 s, consisting of SSFSE sequences at the esophageal body, was obtained during 30-s water swallowing, followed by rest for 10 s at the confirmed slice angle. Esophageal fMRI was then performed using a Fast Imaging Employing Steady-state Acquisition (FIESTA) sequence, under the following settings: TR 3.5 ms, TE 1.5 ms, Flip angle 40°, Bandwidth 125, Frequency 256, Phase 256, FOV 35.0 cm, Slice thickness 8 mm, and Asset sense factor 1.5. Additional images were obtained using the same protocol at the level of the LES.

### Image interpretation

The morphological evaluation included the presence and extent of esophageal dilation (maximal diameter), tortuous changes, and the presence or absence of tumorous lesions. The esophageal motility was expressed by the following parameters: esophageal peristalsis, swallow-induced LES relaxation, presence of simultaneous waves and the esophageal clearance. The obtained images were interpreted by one independent radiologist who was blinded to the results of the other imaging studies and physiological tests.

### *Morphology*

1. *Esophageal dilation* the maximal diameter of the esophagus was measured on the axial SSFSE images, and esophageal dilation was defined as an esophageal diameter >3.5 cm.
2. *Tortuous esophagus* the center of the esophagus was plotted at each level with axial SSFSE images.

Esophageal meandering was defined on the basis of shifted plots over the esophageal radius.

3. *Tumorous lesions* neoplasms responsible for dysphagia or esophageal dilatation, including esophageal and extra-esophageal lesions.

#### Motility

1. *Simultaneous waves* defined when both the anterior and posterior walls of the esophagus seemed to twitch several times at the pleural sites on FIESTA images of the esophageal body.
2. *Esophageal clearance* FIESTA images of the esophageal body were obtained with a clear liquid swallow. When the entire liquid volume entered the stomach, the esophageal clearance was labeled as “good” clearance; otherwise, it was defined as “poor” clearance.
3. *Peristalsis* both SSFSE and FIESTA images of the esophageal body were obtained under continuous liquid swallow. When the esophagus showed contractions and relaxations in response to swallowing, and the intra-esophageal liquid moved into the stomach at the same time, peristalsis was regarded as “positive”; otherwise it was considered to be “negative”.
4. *Impaired LES relaxation* this was diagnosed by the absence of timely/complete distension of the esophageal lumen above the esophagogastric junction following swallowing.

#### Numerical indices

Three healthy male subjects (median age 34, range 33–35 years) underwent fMRI using the above protocols. The following two indices were applied for a more objective and precise evaluation of the esophageal peristalsis and LES relaxation.

#### LFI for peristalsis

The diameter of the esophageal body was continuously measured for 20 s using SSFSE at the level of two-vertebra-length region from cranium to the diaphragm. The minimal diameter was first determined by reviewing 20 of the obtained sequences. Each diameter at every second was then divided by the minimal diameter and was expressed as the “diameter ratio.” The maximal diameter ratio (Rmax) and standard deviation value of all 20 ratios (SDratio) were calculated. The luminal fluctuation index (LFI) was defined by the following formula:  $LFI = R_{max} \times SD_{ratio}$ . The larger the degree and the higher the frequency of contraction and relaxation motility of the esophagus were, the

higher the LFI score was. The presence/absence of esophageal peristalsis was determined by comparing the LFI between patients and normal subjects.

#### Dd/Ds for LES relaxation

The changes in the esophageal diameter were measured at the level of the LES using both SSFSE and FIESTA sequences. The “Dd” and “Ds” were defined as the maximal and minimal diameters during the liquid swallow, respectively.

#### Safety of fMRI

Any adverse events related to fMRI and the time required to complete the fMRI study were recorded. All adverse events were evaluated based on the Common Terminology Criteria for Adverse Events (CTCAE) version 4.

#### Statistical analysis

Data were expressed as the median (range) values. The Wilcoxon paired signed rank test was used to compare the LFI and Dd/Ds between patients and healthy volunteers. The analysis was carried out with the JMP version 8.0 software program (SAS Institute Inc., Cary, NC), and a two-sided  $p$  value  $<0.05$  was considered to be significant.

#### Results

Table 1 shows the demographics of the 11 patients with suspected achalasia and the initial work-up findings based on esophagography, EGD and chest/abdominal CT. The time from onset to final diagnosis ranged from two to 24 years (median seven years). Seven patients had received treatment for dysphagia before enrollment in the present study with pneumatic balloon dilatation and/or the administration of a calcium channel blocker. The initial work-up showed a dilated-tortuous esophagus in 10 of the 11 patients. No tumorous lesion was detected in any of the patients. Simultaneous waves were detected in three patients by esophagography only. The assessment of the esophageal clearance by esophagography was different from that by EGD. Since all patients had excess residue in the esophagus observed on EGD, they were considered to have poor clearance. Peristalsis and impaired LES relaxation could not be assessed by the initial work-up.

The established diagnosis using manometry was achalasia in 10 patients and a hypertensive LES in one patient. A Laparoscopic Heller-Dor operation was performed in all 10 achalasia patients without any intraoperative complications. The median length of the operation was 191

**Table 1** Patients' demographics and the initial work-up findings using esophagography, EGD and chest/abdominal CT ( $n = 11$ )

Parameters		Number of patients		
Gender, male/female		4/7*		
Age, years		40.0 (27–77)		
Body mass index, kg/m <sup>2</sup>		18.9 (16.5–22.1)		
Duration of symptoms, years		7.0 (2–24)		
Prior treatment				
Yes/no		7/4		
Balloon dilatation		4		
Calcium channel blocker		3		
		Esophagography	EGD	Chest/abdominal CT
Maximal diameter, cm		4.5 (1.8–6.2)		
Dilation	Yes/no	10/1	10/1	10/1
Tortuous changes	Yes/no	10/1	10/1	10/1
Tumorous lesion	Yes/no	0/11	0/11	0/11
Simultaneous waves	Yes/no	3/8		
Esophageal clearance	Good/poor	5/6	0/11	

Data are the number of patients, or the median and range  
EGD  
esophagogastroduodenoscopy

(150–292) minutes, with minimal blood loss. All patients showed rapid postoperative recovery, with complete resolution of their preoperative clinical symptoms. The other remaining patient with a hypertensive LES received medical treatment with amlodipine besilate (10 mg/day), which resulted in partial relief of the dysphagia.

#### Feasibility of fMRI

Table 2 compares the results of the evaluation of each parameter and the diagnosis obtained with fMRI and manometry.

**Table 2** Comparison between functional MRI and manometry

		Functional MRI	Manometry
Maximal diameter, cm		4.5 (1.9–5.4)	
Dilation	Yes/no	9/2	
Tortuous changes	Yes/no	10/1	
Tumorous lesion	Yes/no	0/11	
Simultaneous waves	Yes/no	9/2	10/1
Esophageal clearance	Good/poor	1/10	
Peristalsis	Yes/no	0/11	1/10
LES relaxation	Yes/no	0/7	1/10
Diagnosis			
Achalasia		10	10
Other disease		1 <sup>a</sup>	1 <sup>a</sup>

LES lower esophageal sphincter

<sup>a</sup> This case corresponded to the patient (Case 5) who was finally diagnosed to have a hypertensive LES

#### Morphology

1. *Esophageal dilation* the maximal diameter of the esophagus ranged from 1.9 to 5.4 cm (median 4.5 cm). Nine patients were considered to have esophageal dilation, whereas the maximal diameter was 1.9 cm and 2.9 cm in the other two cases (Case 5 and Case 8, respectively).
2. *Tortuous esophagus* this morphology was observed in all but one patient (Case 5).
3. *Tumorous lesions* no tumor was detected in any of the patients.

#### Motility

1. *Simultaneous waves*: Figure 1 shows the typical findings of simultaneous waves. They were detected in all but two patients (Case 5 and Case 11).
2. *Esophageal clearance*: Poor esophageal clearance was noted in 10 patients. The swallowed liquid remained in the esophagus in all but one patient (Case 5).
3. *Peristalsis*: All patients exhibited aperistalsis.
4. *Impaired relaxation of the LES*: although this could not be assessed in four patients due to severe tortuosity and adverse events such as nausea and vomiting during the MRI scans, impaired relaxation of the LES was evident in the remaining seven patients.

Based on the fMRI findings described above, all but one patient (Case 5) were diagnosed with achalasia. Since Case 5 had normal esophageal morphology and normal clearance, achalasia was ruled out. The manometric findings confirmed that all 10 patients diagnosed with achalasia by fMRI had

the condition. Case 5 was diagnosed with a hypertensive LES based on manometric findings of rhythmic waves, LES relaxation, and a high LES resting pressure.



**Fig. 1** Simultaneous pressure waves were often observed with the FIESTA sequence

#### LFI and Dd/Ds ratio

In the healthy volunteer group, fMRI visualized the movement of the swallowed liquid and contraction-relaxation motility which induced esophageal emptying (Fig. 2). In these subjects, no residual water was detected in the esophagus during fMRI.

#### Changes in the diameter ratio and LFI

Figure 3 shows the changes in the “diameter ratio” and LFI value in healthy volunteers and patients. The plotted data clearly show that there were marked changes in the esophageal diameter at rest in healthy volunteers compared with the patients with achalasia. The median LFI of the healthy group was 1.50 (range 1.13–1.73), which was significantly higher than that of the patients (median 0.08, range 0.03–0.25,  $p < 0.05$ ). Thus, the diameter ratio allowed the diagnosis of aperistalsis in all 11 patients.

#### Dd/Ds ratio

This ratio was measured on the sagittal fMRI of the normal subjects. In one normal subject, the ratio was also measured on the axial images. In the three normal subjects in

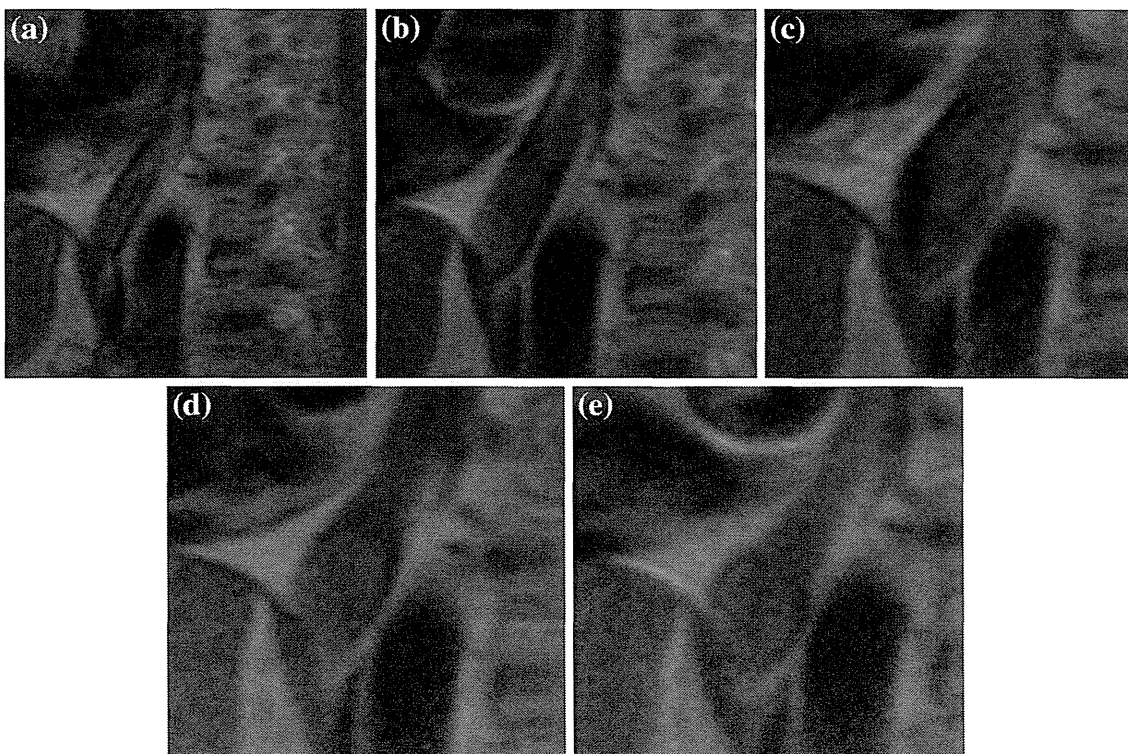


**Fig. 2** Functional MRI allowed the visualization of the movement of the swallowed liquid and esophageal contraction-relaxation motility, which induced esophageal emptying in the normal subjects group

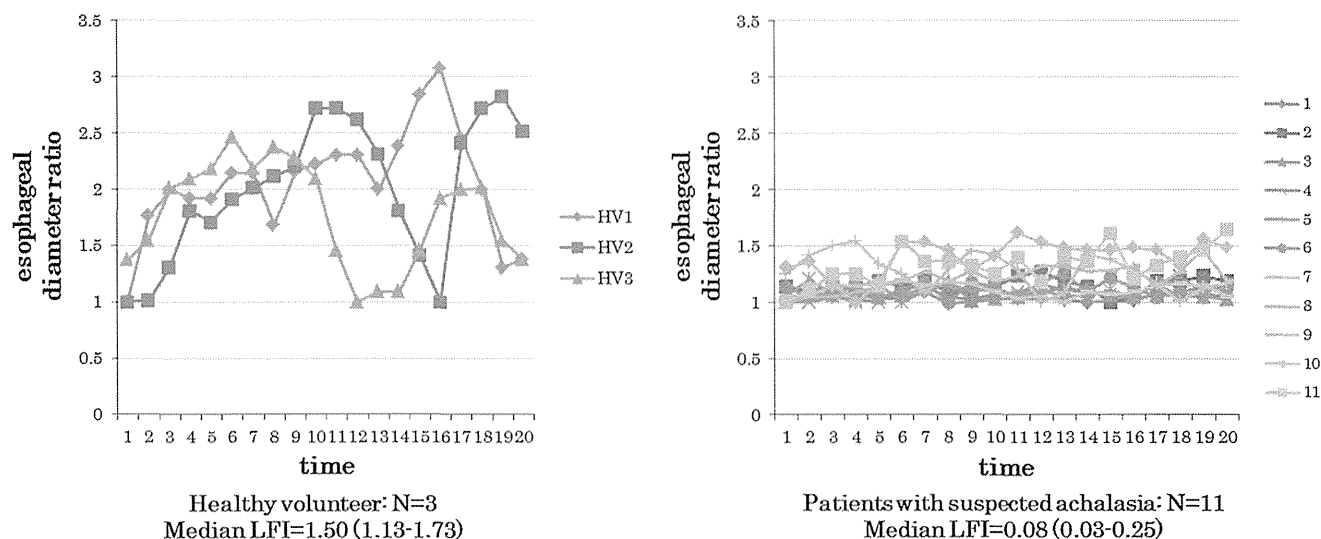


**Fig. 3** The changes in the esophageal diameter ratio and LFI score. *Left* normal subjects, showing esophageal peristalsis, *right* patients with achalasia showed no obvious change in the diameter. The LFI

score of healthy volunteers was significantly higher than that of the patients (Wilcoxon paired signed rank test,  $p < 0.05$ )

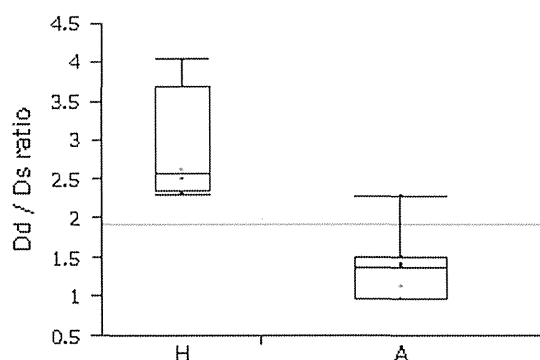


**Fig. 4** *Box-and-whisker* plots of the Dd/Ds ratios in normal healthy subjects (H) and patients with achalasia (A). In these plots, the *lines* within the *boxes* represent median values; the *upper* and *lower lines* of the *boxes* represent the 25th and 75th percentiles, respectively, and the *upper* and *lower bars* outside the *boxes* represent the 90th and 10th percentiles, respectively. ( $p < 0.05$ , by Wilcoxon paired signed rank test)

whom this variable was measured, the median Dd/Ds ratio was 2.59 (range 2.32–4.05). In the patient group, the images of the sagittal slices were not available from four patients due to the tortuous esophagus. Thus, the Dd/Ds ratio was calculated based on the axial images in seven patients. Since the esophageal lumen remained closed throughout water swallowing in one patient (Case 8) and the estimated diameter was 0.0 cm, the Dd/Ds ratio of this patient was considered to be 1.00. The median Dd/Ds ratio of the seven patients (1.40, range 1.00–2.30) was significantly lower than that of the control subjects ( $p < 0.05$ , Fig. 4). These measurements indicated the lack of LES relaxation in all seven patients.

#### Safety of fMRI

No severe side effects (corresponding to more than grade 3 in the CTCAE criteria) were observed in any of the subjects. While no adverse events were recorded in the healthy subjects, several grade 1 events were reported by patients with achalasia, including chest pain, nausea, and vomiting. The time taken to complete the fMRI study was about 30 min.

#### Discussion

The main symptoms of achalasia are dysphasia, chest pain, and backache (so called “achalasia pain”). Although such symptoms are suggestive of achalasia, the diagnosis is often not established for two to three years from the appearance of symptoms [5]. EGD is often the first test used to evaluate dysphasia of esophageal origin and can show esophageal dilation, retention of food or fluid, and a closed LES with a puckered appearance after air insufflation. However, patients with early-stage achalasia are unlikely to show any of the above symptoms, and resistance at the esophagogastric junction may be misinterpreted as peptic stricture, especially when the preliminary diagnosis is GERD [12]. Eckardt et al. [6] stated that the early diagnosis of achalasia could be enhanced if all patients with dysphasia and normal endoscopic findings had their X-rays re-viewed by a second observer and if manometry was performed in cases with equivocal or negative results. On the other hand, additional tests are rarely recommended for patients with normal findings at the first examination.

The use of fMRI to improve the temporal and spatial resolution has recently been proposed for the digestive system, especially for the abdominal cavity. Ajaj et al. [13] reported that gastric peristalsis could be assessed by fMRI using the “gastric motility index”. They compared this index in normal subjects and patients with gastric paresis. More recently, several groups used fMRI to evaluate esophageal peristalsis, LES relaxation and clearance [10]. However, several problems currently hinder the use of fMRI for the assessment of esophageal motility, mainly due to the unique anatomy and physiology of the esophagus. These include its very thin wall, frequent presence of collapsed walls, low-wave amplitudes and higher peristaltic velocity compared with the stomach [13, 14]. To resolve these problems, special contrast media, such as gadolinium-based agents or a ferric ammonium citrate-based solution, were used in previous studies [9–11]. Unfortunately, these types of media cannot be used in patients with dysphagia due to the risk of aspiration.

The present study is the first to describe the potential usefulness of esophageal fMRI with a clear liquid swallow for the diagnosis of achalasia, using several parameters specific to achalasia, and reporting novel indices for diagnosing achalasia. Since any diagnostic modality must be safe and convenient, it is preferable to adopt clear liquid and easy-to-use image sequences. These two points encouraged us to utilize two types of fMRI sequences, SSFSE and FIESTA, which employ T2-weighted images, and which are frequently used in the thoracic field. Since SSFSE has two merits (i.e., small artifacts and good temporal resolution), this sequence is suitable for imaging esophageal wall movements. Furthermore, the FIESTA sequence, which is commonly used in the field of cardiac and macrovascular diseases, shows a higher intensity level of clear liquid in the esophagus. Accordingly, it allows for clearer images of the swallowed water and changes in the esophageal wall elicited by the passage of water to be observed. Thus, the FIESTA images resemble barium esophagography and are appropriate for examining the esophageal lumen morphology and esophageal clearance.

In this study, several parameters specific to achalasia and numerical indices for an objective evaluation were adopted. They allowed for a comparison of the diagnostic ability of different parameters. Table 2 shows the results of the evaluation of each parameter and its usefulness for the diagnosis, with a comparison to the results of manometry. The morphological assessment by fMRI was comparable to that of the initial work-up when using the following parameters: dilation, tortuosity, and the presence or absence of an esophageal tumor. The motility was examined using four parameters. The sensitivity in the diagnosis using simultaneous waves was superior to that of esophagography and was similar to that of manometry, probably

due to the longer observation time and retention of a larger amount of the contrast medium in the esophagus. With regard to the evaluation of esophageal clearance, fMRI obtained with the subject in the supine position more clearly demonstrated poor esophageal clearance in patients with achalasia, compared with esophagography in the standing position. This probably explains the larger number of patients diagnosed with poor clearance by fMRI (10 cases) compared with esophagography (six cases). The results of the assessment of peristalsis and impaired relaxation of the LES by fMRI were similar to those by manometry, with the exception of one patient (Case 5), and the reason(s) for the discrepancy in this case remains unknown. In addition to its diagnostic ability, fMRI is both safe and free of serious side effects. Although more than half of the patients with achalasia reported nausea and one patient suffered vomiting, none developed aspiration pneumonia.

Although a few previous reports assessed the esophageal peristalsis and LES relaxation by fMRI [9–11, 15], these evaluations were subjective and qualitative. In the present study, however, we used two novel objective indices; the LFI and Dd/Ds ratio. The use of cutoff values for the LFI and Dd/Ds ratio allowed us to diagnose aperistalsis and impaired LES relaxation in patients with achalasia. Therefore, the use of the “diameter ratio” and the above indices allows for the objective and semi-quantitative assessment of esophageal motility.

Table 3 provides the results of the comparative analysis of the diagnostic ability of each modality. The conventional modalities, such as esophagography, EGD and chest/abdominal CT, are mainly used for morphological assessment, not the functional analysis. Although esophagography is beneficial for evaluating the esophageal clearance using the “timed-barium esophagography” technique [16], it did not provide an adequate assessment of the esophageal peristalsis and LES relaxation. Patients with dysphagia are initially examined by these modalities, which can rule out the presence of tumorous lesions. However, negative findings with typical morphological features are not uncommon in early-stage achalasia. In addition, repeated esophagography/CTs are associated with a higher risk of radiation exposure. In contrast, fMRI can provide simultaneous morphological and functional evaluation without any risk of radiation. fMRI is thus considered to be potentially useful in the assessment of patients with dysphagia.

Further studies are needed to refine our sequences and imaging protocols to allow for the differentiation of achalasia from other esophageal functional diseases, such as hypertensive LES, diffuse esophageal spasm, nutcracker esophagus, and nonspecific esophageal motility disorders. At present, the differential diagnosis of esophageal functional motility disorders requires manometric recording. It



15. Koyama T, Umeoka S, Saga T, Watanabe G, Tamai K, Kobayashi A, et al. Evaluation of esophageal peristalsis in patients with esophageal tumors: initial experience with cine MR imaging. *Magn Reson Med Sci.* 2005;4:109–14.
16. Vaezi MF, Baker ME, Achkar E, Richter JE. Timed barium oesophagram: better predictor of long term success after pneumatic dilation in achalasia than symptom assessment. *Gut.* 2002;50:765–70.

# A novel endoscopic submucosal dissection technique with robust and adjustable tissue traction

## Authors

Masashi Hirota<sup>1,2,\*</sup>, Motohiko Kato<sup>3,\*</sup>, Makoto Yamasaki<sup>1</sup>, Naoki Kawai<sup>2</sup>, Yasuhiro Miyazaki<sup>1</sup>, Takuya Yamada<sup>3</sup>, Tsuyoshi Takahashi<sup>1</sup>, Tetsuo Takehara<sup>2</sup>, Masaki Mori<sup>1</sup>, Yuichiro Doki<sup>1</sup>, Kiyokazu Nakajima<sup>1,2</sup>

## Institutions

Institutions are listed at the end of article.

submitted 8. July 2013  
accepted after revision  
12. July 2013

## Bibliography

DOI <http://dx.doi.org/10.1055/s-0034-1364879>  
Published online: 28.1.2014  
Endoscopy 2014; 46: 499–502  
© Georg Thieme Verlag KG  
Stuttgart · New York  
ISSN 0013-726X

## Corresponding author

**Kiyokazu Nakajima, MD, FACS**  
Division of Collaborative  
Research for Next Generation  
Endoscopic Intervention  
(Project ENGINE) The Center for  
Advanced Medical Engineering  
and Informatics  
Osaka University  
408-2, Building A  
2-1, Yamadaoka  
Suita, Osaka 565-0871  
Japan  
Fax: +81-6-68760550  
knakajima@gesurg.med.  
osaka-u.ac.jp

**Background and study aims:** A novel esophageal endoscopic submucosal dissection (ESD) technique was devised using a newly developed overtube to achieve adequate tissue traction. The aim of this study was to evaluate the feasibility and safety of this new full-traction ESD (tESD) technique.

**Methods:** The key feature of tESD is tissue traction by grasping forceps, which is passed through the built-in side channel of the overtube. The strength and direction of traction is controlled by rotating the overtube and by adjusting its depth. The en bloc resection rate, procedure time, adverse events, and dissected area per minute were eval-

uated in a porcine model (n=10) and compared with those of conventional ESD (n=10).

**Results:** tESD provided robust and adjustable tissue traction during the procedure. En bloc resection was accomplished in all lesions with no complications. Median procedure time was similar to that of the conventional technique (25 vs. 27 minutes;  $P=0.4723$ ) but the submucosal injection catheter was used less often (1.5 vs. 6;  $P<0.01$ ).

**Conclusions:** tESD might contribute to more efficient esophageal ESD by providing adequate tissue traction. This inexpensive technique may become an attractive option in esophageal ESD.

## Introduction

Endoscopic submucosal dissection (ESD) in the esophagus is one of the most technically challenging procedures, with high perforation rates compared with the conventional mucosal resection technique, mainly because of inadequate traction/retraction of the mucosal flap [1–4]. In order to resolve this problem, we have devised an alternative ESD technique using a newly developed overtube. In this paper, we describe this full-traction ESD (tESD) technique, and present preclinical results.

## Materials and methods

### The tESD technique

The prototype overtube is equipped with a built-in side channel (3 mm outer diameter), through which a standard grasping forceps is passed in order to provide tissue traction (● Fig. 1). The overtube is designed to be rotated around the endoscope within the esophagus.

Using the overtube, the tESD technique is performed as follows. The procedure is performed by three endoscopy operators: 1) the main operator, who controls the endoscope and energy device; 2) the first assistant, who controls the overtube and grasping forceps through the built-in side channel; and 3) the second assistant who assists the main operator in the use of devices through the endoscope, such as the submucosal injection catheter or electro-surgical devices. After circumferential mucosal incision, the overtube is introduced orally into the esophagus. The main operator orientates the view so that the target lesion is at the bottom of the lumen (6-o'clock position). Next, the first assistant rotates the overtube in order to set the side channel at the 6-o'clock position (bottom of the view). The assistant then introduces fine forceps (FG-14p-1, FG047L-1; Olympus Medical Systems, Tokyo, Japan) through the side channel and grasps the edge of the mucosal flap (● Fig. 2a). The assistant then rotates the overtube until the location of the side channel in the endoscopic view is at the 12-o'clock position (top of the view), keeping the flap grasped during the motion (● Fig. 2b) so that the mucosal flap is also retracted upward to the 12-o'clock position. The submucosal layer is usually clearly identified

\* These authors contributed equally to this work.

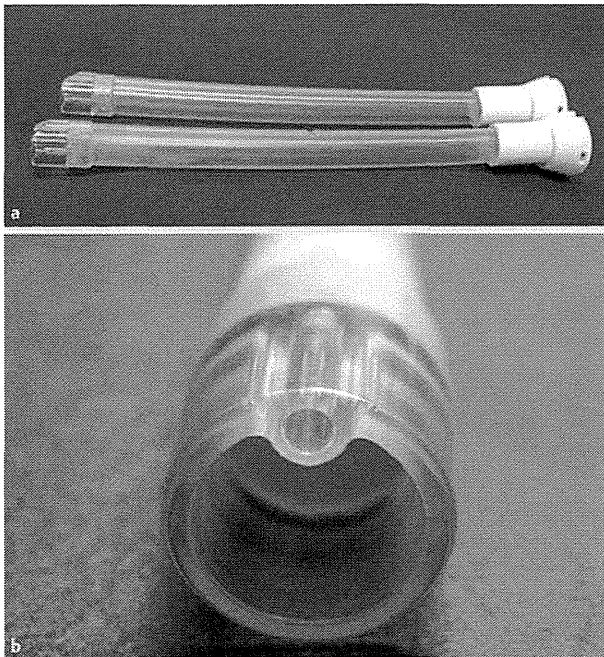


Fig. 1 The prototype overtube. a The whole body. b The side channel.

without the need for submucosal injection, and the main operator dissects it using the SB knife Jr (Sumitomo Bakelite Co., Ltd., Tokyo, Japan), which is introduced through the channel of the scope.

Traction direction can be adjusted from side to side by adjusting the rotation angle of the overtube. Moreover, traction is also adjustable in the direction of the long axis; traction to the oral side is achieved by pulling the forceps back (● Fig. 2c), and traction to the anal side is attained by pushing it through the lumen (● Fig. 2d). The operator instructs the first assistant on where to retract the mucosal flap and then has only to make small adjustment of the scope in order to introduce the SB knife to the dissecting point, where adequate flap retraction has already provided clear visualization of the submucosal layer. Through repetition of these processes, submucosal dissection can be completed (● Video 1).

#### Evaluation of the tESD technique in a porcine model

The feasibility of the technique was evaluated using virtual esophageal lesions in acute porcine models following protocol approval from the Institutional Animal Care and Use Committee. A total of 10 virtual esophageal lesions, 2 cm in diameter, were prepared in five female crossbred pigs (35 kg) in accordance

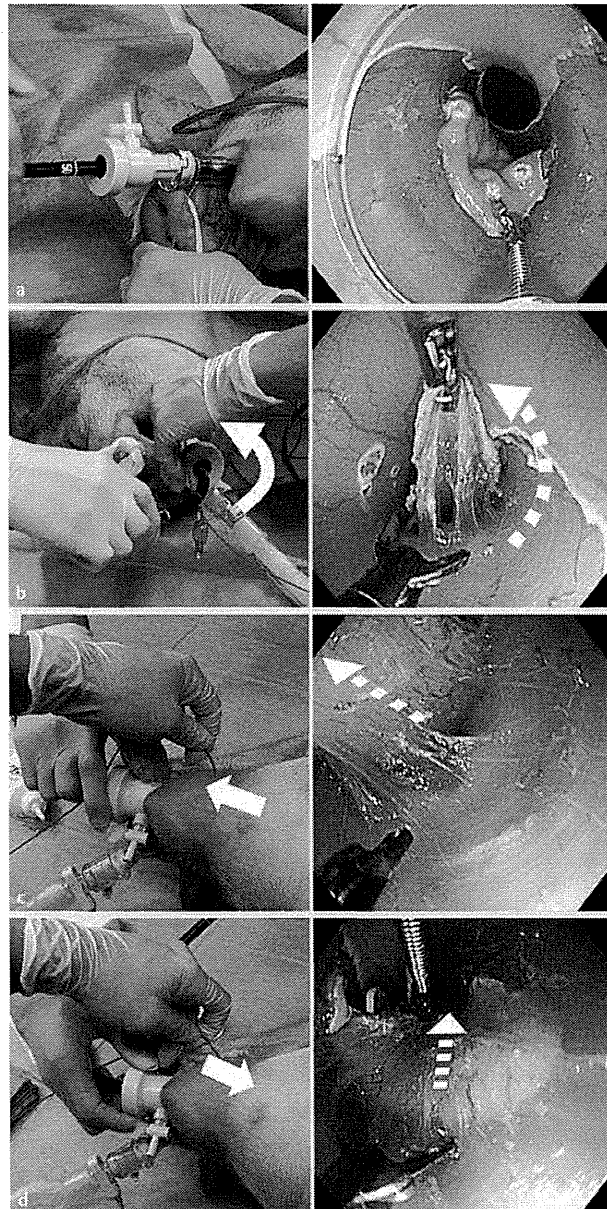
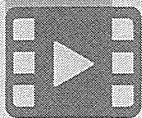


Fig. 2 The technique of full-traction endoscopic submucosal dissection. a Grasping the mucosal flap with forceps. b Traction upwards by rotating the overtube (and hence the forceps and flap) to the 12-o'clock position. c Traction to the oral side. d Traction to the anal side.

with the method described previously (● Fig. 3a) [5]. The completion rate, en bloc resection rate, specimen size, the total ESD time (from mucosal cutting to completion of dissection), intraoperative adverse events, energy device activation time, and number of forceps exchanges were recorded. These measurements were compared with the “control” data obtained from conventional esophageal porcine ESD [5], where a standard commercially available overtube was used in a similar experimental setting: a soft straight distal attachment (D-201-11804; Olympus) was used for submucosal traction/exposure, and a needle knife (DK2618jB-20; Fujifilm, Saitama, Japan) was used exclusively instead of a forceps-type device.

#### Video 1



The technique of full-traction endoscopic submucosal dissection, showing the different traction positions and dissection using the SB knife.



Online content including video sequences viewable at: [www.thieme-connect.de](http://www.thieme-connect.de)

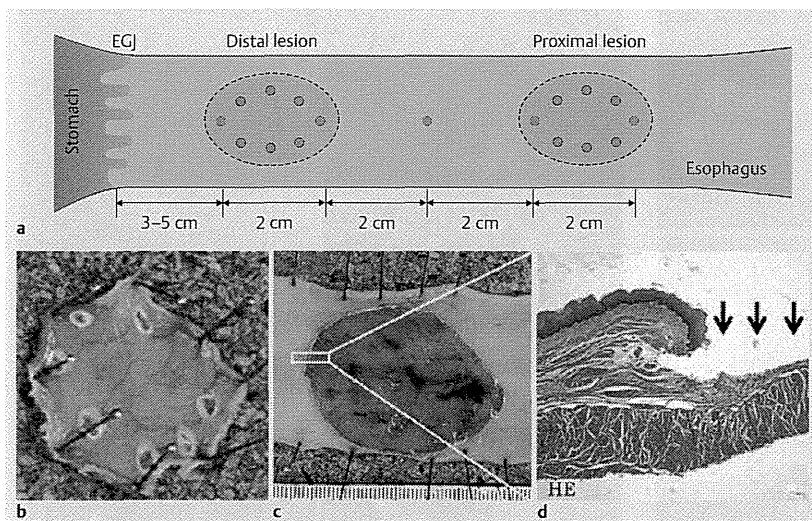


**Fig. 3** Preclinical evaluation of esophageal full-traction endoscopic submucosal dissection in a porcine model. **a** A schematic of virtual lesions. **b** A resected specimen of residual esophagus. **c** Macroscopic view of the esophageal lesion. **d** Microscopic image of the lesion section. Arrows indicate resected area (hematoxylin and eosin). EGJ, esophagogastric junction.

**Table 1** Operative outcomes of endoscopic submucosal dissection.

	tESD (n=10)	Control (n=10)	P value
Completion rate, %	100	100	n.s.
En bloc resection rate, %	100	100	n.s.
Specimen size			
Longest diameter, median (range), mm	28.0 (24–40)	25.5 (20–37)	n.s.
Area, median (range), mm <sup>2</sup>	704 (400–1560)	459 (396–1036)	n.s.
Total procedure time, median (range), minutes	25 (12–50)	27 (22.5–45)	n.s.
Dissected area per minute, median (range), mm <sup>2</sup>	0.47 (0.26–1.01)	0.30 (0.18–0.47)	0.0173
Complications, n	1*	0	n.s.
Energy device			
Total activation time, median (range), seconds	390.5 (179–508)	336 (204–656)	n.s.
Use of cut mode, median (range), n	252 (149–484)	89 (52–203)	0.0004
Use of coagulation mode, median (range), n	171.5 (96–441)	215.5 (152–506)	n.s.
Forceps			
Exchange of items, median (range), n	4 (1–13)	13.5 (4–26)	0.0019
Use of homeostatic forceps, median (range), n	0 (0–3)	1 (0–4)	n.s.
Use of submucosal injection catheter, median (range), n	1.5 (0–4)	6 (1–11)	0.0029

n.s., not significant; tESD, full-traction endoscopic submucosal dissection.

\* Injury to deep muscle layer.

Data were analyzed using statistical software (JMP 10; SAS Institute Inc., Cary, North Carolina, USA), and a *P* value of <0.05 was considered to be significant.

**Results**

Outcomes are summarized in **Table 1**. All 10 virtual esophageal lesions were resected en bloc using the tESD technique, with adequate margins (**Fig. 3b–d**). The median procedure time required for tESD was similar to that for conventional ESD (25 vs. 27 minutes). The area dissected per minute was significantly larger in the tESD group (0.47 vs. 0.30 mm<sup>2</sup>; *P*=0.0173). One injury to the deep muscle layer occurred in one tESD case during mucosal precutting around the markers, before the overtube was set and mucosal dissection was started. No other adverse events from the use of the overtube or the dissecting procedure were experienced. Total activation length of the energy device was similar with both methods, although the number of cut mode activations was significantly greater in the tESD group (252 vs. 89; *P*=0.0004). tESD required fewer device exchanges and less use of

the submucosal injection catheter compared with the conventional group (*P*<0.005).

**Discussion**

Adequate tissue traction is always key to the success of any kind of advanced endoscopic intervention [3]. A variety of traction devices such as the small-caliber tip transparent hood [6], the magnetic anchor [7], external grasping forceps [8], the peroral traction method [9], the pulley method [10], and the cross-counter technique [3] have been reported, but none of them could achieve genuine optimal tissue traction that is independent of the endoscope. Even dual-channel endoscopes only provide “in-line” tissue traction, which is totally dependent on the optical axis. We therefore developed the overtube with a built-in side channel, which could be rotated around the endoscope. This allows adjustable tissue manipulation that is totally independent of endoscope handling. In the current study, feasibility and safety of the tESD technique were confirmed. The prototype demonstrated expected perform-

ance and tESD was accomplished in all lesions with no adverse events. In the comparison with historical outcomes from conventional ESD, we found two interesting results, which possibly suggest improved safety and dissection efficacy with tESD. The first was that the submucosal injection catheter was used less often during tESD. This would indicate that the surgeon had a clear visualization of the submucosal layer and could identify the muscle layer exactly and keep to the appropriate dissection line without the need for submucosal injection. The other observation was that the “cut mode” was used more frequently during tESD than during conventional ESD. This might suggest that the surgeon was able to choose the most appropriate energy device due to the clear view of the submucosal layer and associated vessels. In this limited experimental model, there was no significant difference between the two techniques in outcomes such as procedure time, en bloc resection rate, and complication rate. However, these outcomes may be enhanced if further studies with an increased learning curve were conducted.

Another interesting observation from using the tESD technique relates to the division of work between the main endoscopy surgeon who controls the scope and uses the cutting or dissecting devices and the first assistant who organizes surgical exposure with tissue traction/retraction. This brings us some benefit over the conventional “solo” technique, as the main surgeon can concentrate on handling the endoscope and managing the energy device. This shared working could not only improve the safety of the procedure, but also contribute to education and training in the technique.

The feasibility/safety and potential efficacy of the tESD technique using a prototype device have been demonstrated. However, this was an animal Phase I study with a relatively small sample size. A human prospective randomized study would be necessary to demonstrate a genuine advantage and significance of the tESD technique.

### Conclusion

The study revealed that the tESD technique potentially contributes to safe and efficient ESD by providing robust and adjustable tissue traction. This inexpensive technique may become an attractive option in standardizing technically demanding endoscopic interventions.

**Competing interests:** None.

### Institutions

- <sup>1</sup> Department of Gastroenterological Surgery, Osaka University Graduate School of Medicine, Osaka, Japan
- <sup>2</sup> Division of Collaborative Research for Next Generation Endoscopic Intervention (Project ENGINE), The Center for Advanced Medical Engineering and Informatics, Osaka University, Osaka, Japan
- <sup>3</sup> Department of Gastroenterology and Hepatology, Osaka University Graduate School of Medicine, Osaka, Japan
- <sup>4</sup> Department of Gastroenterology, Osaka Police Hospital, Osaka, Japan

### Acknowledgment

▼

A part of this work was presented at Digestive Disease Week 2013 (Orlando, Florida, USA).

The work was carried out under the grant of “Strategic Foundational Technology Improvement Support Operation” (2009–2012) and “Program to Support Development of Medical Equipment and Devices to Solve Unmet Medical Needs” (2012–2013), from The Ministry of Economy, Trade, and Industry, Japan.

We acknowledge Kohan (Kobe, Japan) for manufacturing the new overtube prototype.

### References

- 1 Othman MO, Wallace MB. Endoscopic mucosal resection (EMR) and endoscopic submucosal dissection (ESD) in 2011, a Western perspective. *Clin Res Hepatol Gastroenterol* 2011; 35: 288–294
- 2 Matsui N, Akahoshi K, Nakamura K et al. Endoscopic submucosal dissection for removal of superficial gastrointestinal neoplasms: a technical review. *World J Gastrointest Endosc* 2012; 4: 123–136
- 3 Okamoto K, Okamura S, Muguruma N et al. Endoscopic submucosal dissection for early gastric cancer using a cross-counter technique. *Surg Endosc* 2012; 26: 3676–3681
- 4 Deprez PH, Bergman JJ, Meisner S et al. Current practice with endoscopic submucosal dissection in Europe: position statement from a panel of experts. *Endoscopy* 2010; 42: 853–858
- 5 Nakajima K, Moon JH, Tsutsui S et al. Esophageal submucosal dissection under steady pressure automatically controlled endoscopy (SPACE): a randomized preclinical trial. *Endoscopy* 2012; 44: 1139–1148
- 6 Yamamoto H, Kawata H, Sunada K et al. Successful en-bloc resection of large superficial tumors in the stomach and colon using sodium hyaluronate and small-caliber-tip transparent hood. *Endoscopy* 2003; 35: 690–694
- 7 Gotoda T, Oda I, Tamakawa K et al. Prospective clinical trial of magnetic-anchor-guided endoscopic submucosal dissection for large early gastric cancer (with videos). *Gastrointest Endosc* 2009; 69: 10–15
- 8 Imaeda H, Iwao Y, Ogata H et al. A new technique for endoscopic submucosal dissection for early gastric cancer using an external grasping forceps. *Endoscopy* 2006; 38: 1007–1010
- 9 Jeon WJ, You IY, Chae HB et al. A new technique for gastric endoscopic submucosal dissection: peroral traction-assisted endoscopic submucosal dissection. *Gastrointest Endosc* 2009; 69: 29–33
- 10 Li CH, Chen PJ, Chu HC et al. Endoscopic submucosal dissection with the pulley method for early-stage gastric cancer (with video). *Gastrointest Endosc* 2011; 73: 163–167

# Dynamic Article: Steady Pressure CO<sub>2</sub> Colonoscopy: Its Feasibility and Underlying Mechanism

Masashi Hirota, M.D.<sup>1,2</sup> • Yasuhiro Miyazaki, M.D.<sup>1</sup> • Tsuyoshi Takahashi, M.D.<sup>1</sup>  
 Makoto Yamasaki, M.D.<sup>1</sup> • Shuji Takiguchi, M.D.<sup>1</sup> • Masaki Mori, M.D.<sup>1</sup>  
 Yuichiro Doki, M.D.<sup>1</sup> • Kiyokazu Nakajima, M.D.<sup>1,2</sup>

<sup>1</sup> Department of Gastroenterological Surgery, Osaka University Graduate School of Medicine, Osaka, Japan

<sup>2</sup> Division of Collaborative Research for Next Generation Endoscopic Intervention, Center for Advanced Medical Engineering and Informatics, Osaka University, Osaka, Japan

**BACKGROUND:** Steady pressure automatically controlled endoscopy is a new insufflation concept, achieving a laparoscopy-like steady environment in the upper GI tract, recently reported in the esophagus.

**OBJECTIVE:** The purpose of this work was to validate the feasibility and safety of steady pressure automatically controlled endoscopy in the lower GI tract and to identify major factors that enable it.

**DESIGN:** This was a nonsurvival animal study using canine models.

**SETTINGS:** The study was conducted in an academic center.

**PATIENTS:** Canine models were used in this study.

**INTERVENTIONS:** In experiment 1, steady pressure automatically controlled endoscopy was attempted in the cecum with insufflation pressures of 4, 8, and 12 mm Hg. We assessed performance by video review and continuous intracecal pressure monitoring. Next, steady pressure

automatically controlled endoscopy was performed for 20 minutes under optimal pressure, 8 mm Hg (n = 10). In experiment 2, steady pressure automatically controlled endoscopy was attempted in the rectum with or without artificial colonic flexure and with either low (8 mm Hg) or high (16 mm Hg) insufflation pressure to assess the effects of anatomic flexure and insufflation pressure on the establishment of steady pressure automatically controlled endoscopy (n = 6).

**MAIN OUTCOME MEASURES:** We measured multipoint intraluminal pressure monitoring in the upstream bowel, as well as cardiopulmonary parameters.

**RESULTS:** For experiment 1, steady pressure automatically controlled endoscopy in cecum was successful at all of the tested insufflation pressures; 8 mm Hg provided the optimal result. Steady pressure automatically controlled endoscopy was safely performed for 20 minutes at 8 mm Hg without any cardiopulmonary parameter changes or intraluminal pressure elevation in the upstream bowel. For experiment 2, confinement of the steady pressure environment to the rectum was achieved only with the assistance of colonic flexure and at 8 mm Hg insufflation pressure. In other conditions, the insufflated gas extended throughout the entire colon.

**LIMITATIONS:** This study was limited by being an animal study.

**CONCLUSIONS:** Steady pressure automatically controlled endoscopy is feasible and safe in the lower GI tract under the optimized insufflation pressure and in the presence of anatomical flexure (see Video, Supplemental Digital Content 1, <http://links.lww.com/DCR/A150>).

Supplemental digital content is available for this article. Direct URL citations appear in the printed text, and links to the digital files are provided in the HTML and PDF versions of this article on the journal's Web site ([www.dcrjournal.com](http://www.dcrjournal.com))

**Funding/Support:** This work was supported by a research grant from Fujifilm (Tokyo, Japan).

**Financial Disclosure:** Dr. Nakajima received financial support from Fujifilm (Tokyo, Japan).

**Correspondence:** Kiyokazu Nakajima, M.D., Division of Collaborative Research for Next Generation Endoscopic Intervention, Center for Advanced Medical Engineering and Informatics, Osaka University, Suite 0912, Center of Medical Innovation and Translational Research, 2-2, Yamadaoka, Suita, Osaka 565-0871, Japan. E-mail: [knakajima@gesurg.med.osaka-u.ac.jp](mailto:knakajima@gesurg.med.osaka-u.ac.jp)

Dis Colon Rectum 2014; 57: 1120–1128

DOI: 10.1097/DCR.0000000000000190

© The ASCRS 2014

**KEY WORDS:** Colonoscopy; Endoscopy; Insufflation; Steady pressure automatically controlled endoscopy.

Endoscopic submucosal dissection (ESD) has been gradually disseminated as a less invasive treatment for early stage GI cancer. However, colonic ESD is commonly considered difficult because of the anatomic peculiarities of the colon, including its long length, easy expansion, numerous convolutions, and thin wall.<sup>1</sup> Techniques or instruments for endoscopic procedures are limited, and some endoscopic surgeons, including our team, have advocated that a rethinking of the platform for flexible endoscopy is necessary.<sup>2,3</sup>

We have focused attention on insufflation, which is one of the most fundamental parts of the endoscopic procedure because it provides working space.<sup>3,4</sup> Our group recently reported a new modality called steady pressure automatically controlled endoscopy (SPACE),<sup>4</sup> in which a semiclosed system is created in the GI tract to provide a constant pressure environment using an automated CO<sub>2</sub> insufflator, with an overtube and dedicated adapter to prevent gas leakage. We demonstrated that when SPACE is performed in the esophagus, it is possible to create a constant pressure environment with high reproducibility during esophagoscopy. Compared with manual insufflation, SPACE had the advantage of reducing gas migration to the distal bowel. Furthermore, we confirmed that SPACE shortened the time needed for esophageal ESD in a randomized preclinical study.<sup>4</sup>

Steady visualization created by SPACE would help a surgeon recognize the adequate layer to be dissected. This would lessen misidentifying of the submucosal layer and incorrect activation of energy devices and improve the safety of ESD by reducing the risk of perforation, which is reported with a high incidence in lower GI tracts<sup>5,6</sup> with a risk of abdominal compartment syndrome.<sup>7,8</sup> In the event of iatrogenic intestinal perforation during the procedure, SPACE would avoid excess pneumoperitoneum under the control of insufflation pressure. Steady visualization created by SPACE would also improve efficiency of the intervention by helping the surgeon with an immediate grasp of the surgical view. Automatic and rapid recovery of visualization would save the procedure time, especially in a complex situation where endoscopic suction is applied frequently, such as in cases of bleeding or poor preparation. It might also be useful to prevent patient discomfort during and/or long after the procedure caused by the migration of insufflated gas to the proximal bowel.<sup>9–12</sup> However, the feasibility and safety of colonic SPACE remain unclear. Even if it is feasible to use this procedure in the lower GI tract, the degree of gas migration to the upstream bowel and theoretical concern of hypercarbia have been reported in CO<sub>2</sub> insufflation<sup>13–16</sup> and should be examined. In addition, the factors that enable maintenance of a constant pressure environment in the lower GI tract should be identified. The present study seeks to validate the feasibility and safety of SPACE and to examine the factors that facilitate SPACE in the lower

GI tract. To our knowledge, this is the first preclinical study to evaluate SPACE colonoscopy.

## MATERIALS AND METHODS

### Animal Preparation

All of the trials were conducted using acute-phase canine models (male, 10 months old, and 20–25 kg). All of the procedures were performed according to the animal protocol approved by the animal use and care administrative advisory committee of our institution. Food intake was halved from 4 to 2 days before the trials, after which the animals were fasted. Anesthesia was induced by intravenous administration of propofol (5 mg/kg), with endotracheal intubation in the supine position. Ventilation was maintained using a mechanical ventilator (KV-1a; Kimura Medical, Co., Ltd., Tokyo, Japan) with 50% oxygen, 50% N<sub>2</sub>O, and 2% sevoflurane inhalation under a fixed minute volume (respiratory rate, 18 breaths per minute). An intravenous line was placed in the posterior auricular vein to hydrate the animal with a balanced electrolyte solution. CO<sub>2</sub> capnometry (TG-221T, Nihon Kohden, Tokyo, Japan) and portable pulse oximetry (TL-201T, Nihon Kohden) were used to document end-tidal CO<sub>2</sub> and percutaneous oxygen saturation during each session. The left femoral artery was catheterized for blood gas analysis using a handheld blood analyzer (i-STAT, Abbott Point of Care Inc., Princeton, NJ). No antispasmodic agents were used for the GI tract. Fecal residue was endoscopically washed from the colon using an endoscopy water pump (JW-2, Fujifilm, Tokyo, Japan). Each canine was humanely killed on completion of the trial.

### Colonic Insufflation System

To prevent gas leakage from the anus during constant pressure insufflation of the canine colon, a handmade overtube with a check valve function (rectal overtube) was placed into the rectum of each canine (Fig. 1A). A double-channel endoscope (EG-450D5, Fujifilm) was introduced via the rectal overtube into the intestinal tract. A CO<sub>2</sub> insufflation line was connected to 1 channel using a plug (BioShield irrigator, US Endoscopy, Mentor, OH; Fig. 1B). In SPACE, the built-in endoscopic air compressor is turned off; a standard laparoscopic insufflator (UHI-3, Olympus Medical Systems, Tokyo, Japan) was used. During manual insufflation, gas was supplied using a GI CO<sub>2</sub> insufflator (GW-1, Fujifilm) by manipulating the gas-water button according to the endoscopist's observation.

### Continuous GI Intraluminal Pressure Monitoring

Continuous GI intraluminal pressure monitoring was conducted in each experiment, as reported previously.<sup>4</sup> To measure the endoluminal pressure in the GI tract near the tip of the endoscope, we used the free biopsy channel for the dye-spraying catheter (Fine Jet, Top, Tokyo, Japan) as a pressure probe. Then, in the area beyond the point

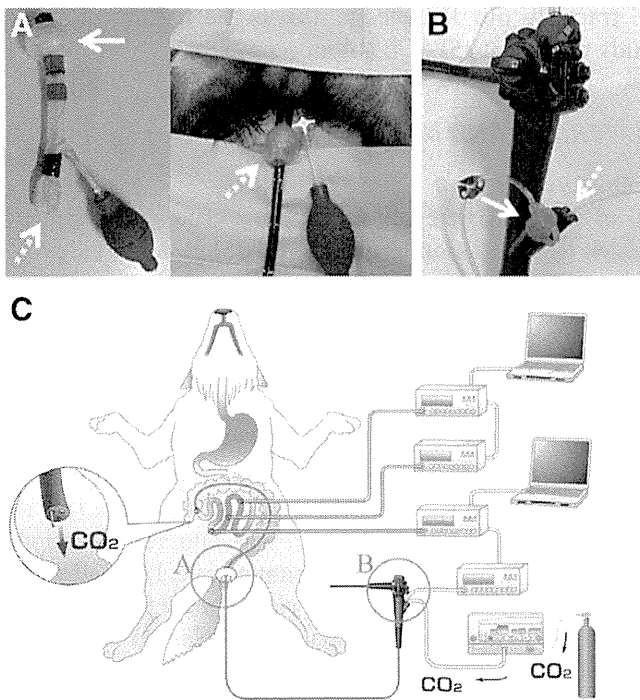


**FIGURE 1.** A, At left, the handmade rectal overtube, a pressure-type balloon at the tip (solid arrow), was wedged into the rectal lumen to prevent leakage while affixing the tube. The tube opening has a vinyl valve structure (dotted arrow) to prevent gas leakage from the slight gap between the overtube and the endoscope. The arrangement had a check valve effect when inverted and fitted to the endoscope. At right, the rectal overtube inserted into the dog and the endoscope inserted into the lower GI tract. B, A close-up of the forceps channels. The insufflation line from the UHI-3 automatic insufflation device is connected to a biopsy channel to perform steady pressure automatically controlled insufflation (solid arrow). A pigment dispersion catheter is inserted into the other channel as a pressure measurement probe in the endoscope tip (dotted arrow). C, The experimental setting for experiment 1, showing continuous multipoint intraluminal pressure monitoring during steady pressure automatically controlled endoscopy (SPACE) in the cecum. Each pressure measurement probe was connected to a digital manometer, and we recorded the intraluminal pressure in the cecum at insufflation sites 50, 100, and 150 cm orally from the ileocecum.

of insufflation at the measurement site, we made a small incision in the intestinal wall via minilaparotomy and placed a polypropylene catheter (2.4 mm diameter, Top) in the gut lumen. After probe placement, the incision was temporarily closed using a sealing device (LapDisc, Hakko Corporation, Tokyo, Japan); each pressure line was delivered extracorporeally through the sealing device. Next, each pressure probe was connected to a digital manometer (MT-210F, Yokogawa, Tokyo, Japan). Pressure measurements (in millimeters of mercury) taken at 1-second intervals were recorded on a dedicated personal computer.

#### Experiment 1 (Cecum Insufflation Study)

The feasibility and safety of SPACE colonoscopy was validated in the cecum, which evaluated the possibility of retrograde gas migration over the ileocecal valve to the upstream bowel, because it is close to the small intestine.

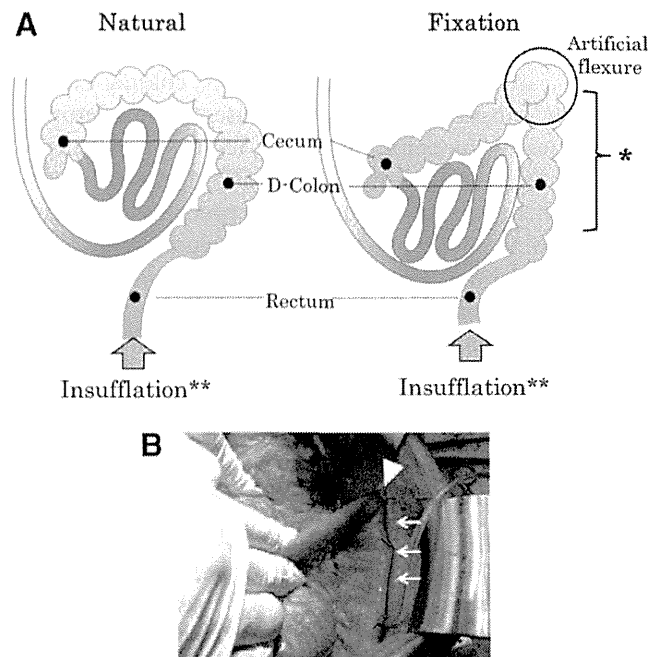


**FIGURE 2.** A, The experimental setting for experiment 2. \*Artificial fixation of the distal colon (D-Colon) to the retroperitoneum. \*\*Insufflation mode was 8- or 16-mm Hg steady pressure automatically controlled endoscopy (SPACE). • Points at which intraluminal pressure was measured. B, The fixation model created in experiment 2. The middle third of the colon is fixed to the retroperitoneum (solid arrow), and an artificial flexure was created (arrowhead).

First, to evaluate the feasibility of cecal SPACE and optimize the insufflation setting, we attempted colonoscopy in the canine cecum ( $n = 3$ ) for 10 minutes with either SPACE or manual insufflation. SPACE was attempted at insufflation pressures of 4, 8, and 12 mm Hg (flow rate, 35 L/min). During manual insufflation, endoscopists were instructed to adjust the insufflation level to maintain the endoscopic view that they believed was most suitable for diagnostic examination. During all of the procedures, intracecal pressure was continuously monitored, and the endoscopic visualization was video recorded for subsequent objective assessment. We also attempted forceful endoscopic suction and evaluated the recovery process of visualization after collapse for each insufflation setting. Eight blinded, board-certified endoscopists (4 gastroenterologists and 4 surgeons) reviewed the videos to assess each insufflation outcome using the following 4-point, 5-scale scoring system: 1) steadiness of visualization, 2) reproducibility of visualization after suction, 3) degree of distension of the lumen, and 4) degree of ease of causing lumen collapse using suction.<sup>4</sup>

Subsequently, we evaluated the safety of cecal SPACE regarding retrograde gas migration and the impact of cardiopulmonary parameters. The pressure probes were placed at 3 points in the ileum (50, 100, and 150 cm orally from the ileocecal valve; Fig. 1C). SPACE colonoscopy was performed in the cecum for 20 minutes ( $n = 10$ ) at the optimized insufflation pressure (8 mm Hg). The impact on

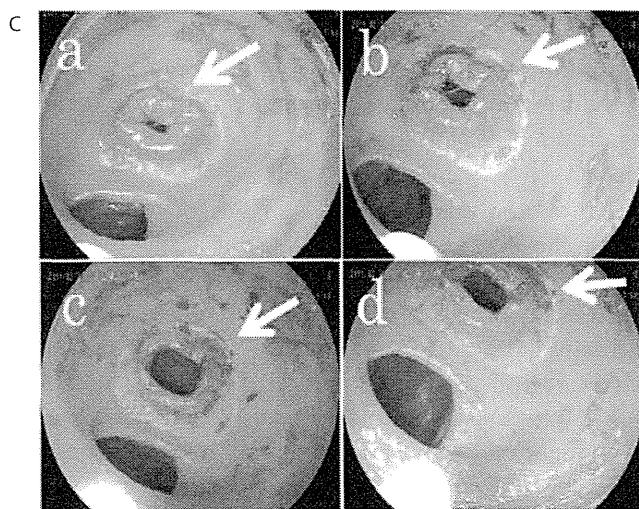
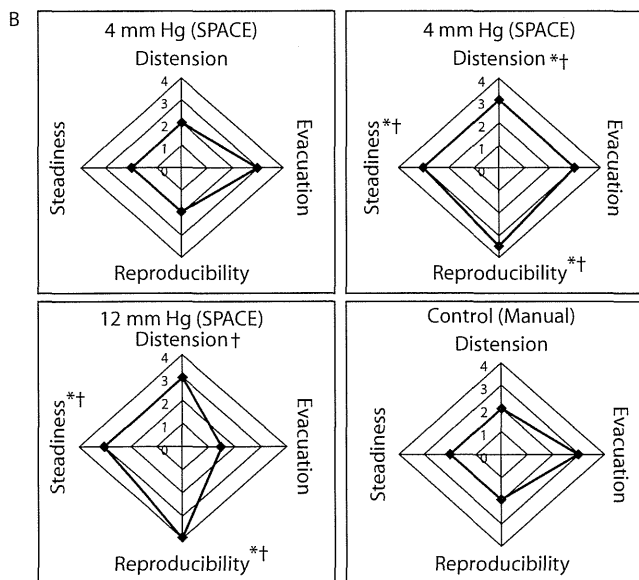
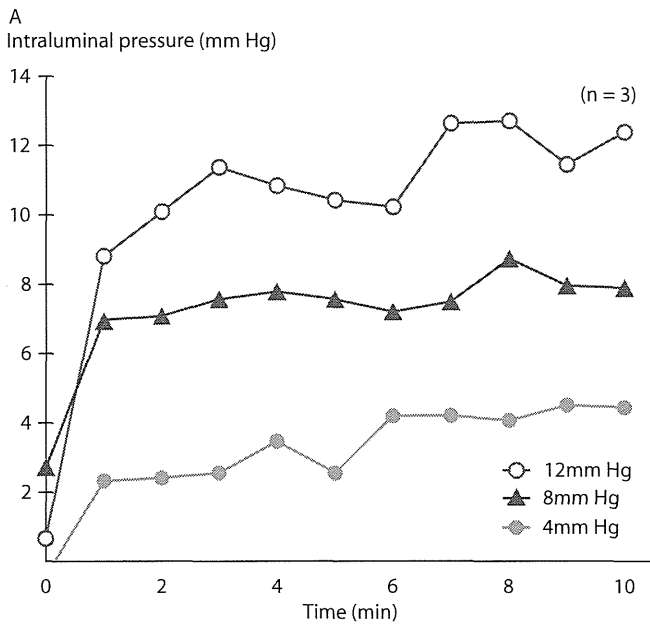


**FIGURE 3.** A, Intracecal pressure changes during steady pressure automatically controlled endoscopy (SPACE; 4, 8, and 12 mm Hg) and in control animals for 10 minutes. B, Endoscopic visualization of each SPACE condition (a, 4 mm Hg; b, 8 mm Hg; c, 12 mm Hg) and the control (d, manual insufflation). The diameter of the ileocecal valve (arrow) during SPACE (a–c) increases as the pressure setting increases. C, Results of a questionnaire based on video review of each insufflation condition by 8 endoscopists. Median values are presented for steadiness of visualization, degree of ease of causing lumen collapse using suction, reproducibility of visualization after suction, and degree of distension of the lumen. Each score was compared among insufflation conditions using the Wilcoxon rank-sum test; \* $p < 0.05$  vs control, † $p < 0.05$  vs 4-mm Hg SPACE).

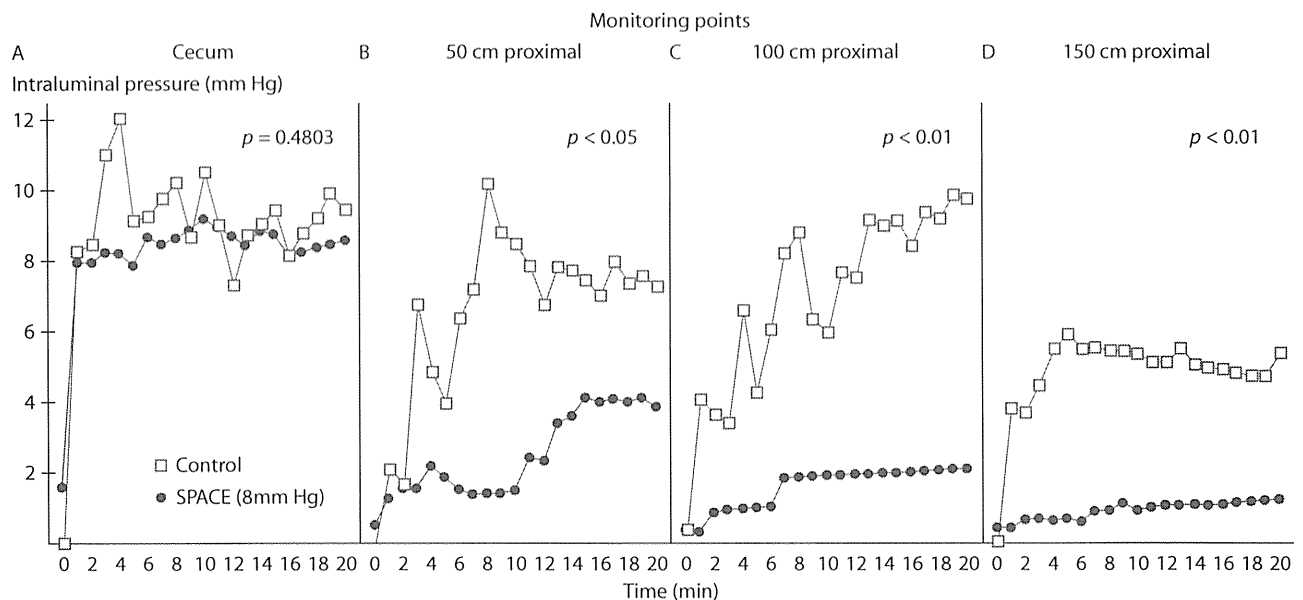


**FIGURE 4.** Intraluminal pressure changes at each monitoring point during steady pressure automatically controlled endoscopy (SPACE; 8 mmHg) and control (manual) for 20 minutes.

the following cardiopulmonary parameters was measured every 5 minutes: 1) blood pressure (in millimeters of mercury), 2) heart rate (beats per minute), 3) percutaneous oxygen saturation (percentage), and 4) end-tidal CO<sub>2</sub>. Additional measurements were obtained for arterial blood gas analysis every 10 minutes, including arterial partial pressure of oxygen (in millimeters of mercury), arterial partial pressure of carbon dioxide (in millimeters of mercury), pH, base excess (in millimoles per liter), and HCO<sub>3</sub><sup>-</sup> (in millimoles per liter). To investigate the differences in the insufflation method, manual colonoscopy was performed in the cecum with CO<sub>2</sub> insufflation using different animals as controls (n = 5), and the same parameters were assessed for comparison. During manual insufflation, endoscopists were instructed to adjust the insufflation level to keep the endoscopic view of the controls as similar as possible to the view of 8-mmHg SPACE in experimental animals, particularly relying on the size of the ileocecal sphincter opening as needed. Other conditions were the same in the control group as in the SPACE group.

#### Experiment 2 (Rectum Insufflation Study)

In a previous trial,<sup>4</sup> we hypothesized that both the presence of intestinal flexure and optimal insufflation pressure might be key factors in establishing upper GI SPACE. Here, we examined how these 2 factors might contribute to successful SPACE colonoscopy.

The canine colon loosely arches between the anus and the cecum without strong fixation to the retroperitoneum (natural models). To examine the impact of presence of flexure on SPACE, we created fixation models by fixing the middle one third of the colon to the retroperitoneum with

6 stitches. These fixation sutures created an artificial flexure resembling the human splenic curve in the proximal segment of the canine bowel (Fig. 2). To evaluate the impact of optimal insufflation pressure, we used either high-pressure insufflation (16 mmHg) or optimal-pressure insufflation (8 mmHg). The flow rate was fixed at 35 L/min in both models.

Two pressure probes were placed in the cecum and the descending colon (n = 6). Next, rectal SPACE was attempted for 15 minutes in fixation or natural models, with high-pressure (16-mmHg) or optimal-pressure (8-mmHg) insufflation in the rectum (Fig. 2). The success of rectal SPACE in this experiment was defined as the establishment of a constant pressure environment that was confined to the rectum, without massive gas migration beyond the insufflated segment (the rectum). Gas migration was also monitored with sporadic x-ray images during and immediately after insufflation for each condition.

#### Statistical Analysis

All of the data were analyzed using a statistical software package (JMP 10, SAS Institute Inc., Cary, NC) on a universal personal computer. ANOVA was used to compare parametric data, and the Wilcoxon rank-sum test was applied to nonparametric data. The Wilcoxon signed-ranks test was used for paired comparisons within changes of cardiopulmonary and arterial blood gas parameters. A *p* value <0.05 was considered statistically significant.

**Table 1** Changes of cardiopulmonary and arterial blood gas parameters after 20 minutes of CO<sub>2</sub> insufflation

Variable		SPACE (N = 10)		Control (N = 5)		<i>p</i> <sup>2</sup>
		Data	<i>p</i> <sup>1</sup>	Data	<i>p</i> <sup>1</sup>	
Blood pressure, median (range), mm Hg	Pre	71.8 (57.7–94.3)	0.2801	64.7 (60.3–74.0)	0.4256	0.2715
	Post	81.5 (53.7–94.3)		64.7 (52.3–77.0)		
Heart rate, median (range), beats per min	Pre	118 (101–160)	0.9004	115 (84–121)	0.7500	0.7873
	Post	121 (99–157)		110 (88–121)		
Respiratory rate, median (range), beats per min	Pre	18 (18–29)	1.0000	18 (18)	1.0000	0.6030
	Post	18 (18–29)		18 (18)		
SpO <sub>2</sub> , median (range), %	Pre	100 (99–100)	1.0000	100 (95–100)	1.0000	0.2683
	Post	100 (100)		100 (98–100)		
EtCO <sub>2</sub> , median (range), mm Hg	Pre	32.5 (190–380)	0.1875	29.0 (20.0–36.0)	0.0625	0.1430
	Post	340 (29.0–39.0)		34.0 (26.0–39.0)		
pH, median (range)	Pre	7.26 (7.25–7.31)	0.1934	7.32 (7.23–7.36)	0.0625	<b>0.0020</b>
	Post	7.25 (7.23–7.31)		7.27 (7.12–7.32)		
PaO <sub>2</sub> , median (range), mm Hg	Pre	255 (176–360)	0.8457	239 (207–278)	0.0625	0.4224
	Post	252 (209–367)		244 (229–292)		
PaCO <sub>2</sub> , median (range), mm Hg	Pre	52.5 (45.4–55.7)	0.2324	45.9 (42.0–48.3)	0.0625	<b>0.0037</b>
	Post	53.7 (50.1–57.8)		53.7 (47.7–61.1)		
HCO <sub>3</sub> <sup>-</sup> , median (range), mmol/L	Pre	24.1 (22.8–27.9)	0.3066	23.0 (19.9–25.0)	0.5000	0.5921
	Post	24.3 (22.9–27.5)		22.1 (19.7–25.9)		
BE, median (range), mmol/L	Pre	-3.0 (-4.0–2.0)	1.0000	-3.0 (-8.0 to -1.0)	0.5000	0.1207
	Post	-3.0 (-4.0–1.0)		-5.0 (-10 to -1.0)		

Boldface indicates significance. Each parameter was analyzed using a paired design and the Wilcoxon signed-rank test ( $p < 0.05$  was considered the threshold for statistical significance). *p*<sup>1</sup> shows comparison before and after the insufflation trial (Pre vs Post); *p*<sup>2</sup>, comparison of changes before and after the insufflation trial with respect to different insufflation methods (SPACE vs control).

BE = base excess; EtCO<sub>2</sub> = end-tidal CO<sub>2</sub>; PaCO<sub>2</sub> = arterial partial pressure of carbon dioxide; PaO<sub>2</sub> = arterial partial pressure of oxygen; SPACE = steady pressure automatically controlled endoscopy; SpO<sub>2</sub> = percutaneous oxygen saturation.

## RESULTS

### Experiment 1

SPACE was feasible in the cecum in all of the animals. With our SPACE system, the intracecal pressure quickly reached each preset value (4, 8, and 12 mm Hg), with minimal pressure fluctuation (Fig. 3A). Endoscopic visualization revealed that the lumen distended immediately after initiating insufflation, and a stable view was maintained (Fig. 3B). In the questionnaire on endoscopic visualization and suction, all of the items except evacuation scored higher for 8- and 12-mm Hg SPACE than for 4-mm Hg SPACE and the control (Fig. 3C). In contrast, 12-mm Hg SPACE tended to be scored lower because of difficulty in evacuation (see Video, Supplemental Digital Content 2, which demonstrates SPACE, <http://links.lww.com/DCR/A151>). Because all of the items scored high at 8 mm Hg, it was considered the optimal pressure setting for cecal SPACE. Therefore, we adopted 8 mm Hg in the subsequent 20-minute SPACE insufflation trials.

SPACE resulted in no major gas migration to the upstream bowel. The details of pressure profiles are shown in Figure 4. Intraluminal pressure in the cecum (which was the insufflation area) reached the preset value immediately after the commencement of SPACE, after which minute fluctuations in width were observed (mean total measurement, 8.18 ± 2.53 mm Hg). The mean measurement with manual

insufflation was 8.94 ± 4.07 mm Hg, and although the vertical fluctuations were greater than those with SPACE, we observed no difference in cecal pressure changes between SPACE and manual insufflation (Fig. 4A). Almost no increase in ileal pressure was noted at 50, 100, and 150 cm orally from the ileocecal valve, and each intraluminal pressure on completion (at 20 minutes) remained low (3.88 ± 2.75, 2.12 ± 2.23, and 1.25 ± 1.36 mm Hg). Over time, pressure changes at all 3 of the ileum sites were significantly lower than the intracecal pressure during SPACE ( $p < 0.0001$ ). In contrast, during manual insufflation, intraileal pressure at 50, 100, and 150 cm from the ileocecal valve increased early after the commencement of insufflation, and at completion (at 20 minutes) the intraluminal pressures were 7.32 ± 7.05, 9.77 ± 5.11, and 5.42 ± 5.53 mm Hg. When we compared pressure changes over time, they were significantly lower during SPACE than during manual insufflation (Figs. 4B–D).

Neither SPACE nor manual colonoscopy in the cecum resulted in any negative effects on cardiopulmonary parameters (Table 1). No statistically significant changes in blood pressure, heart rate, respiratory rate, percutaneous oxygen saturation, end-tidal CO<sub>2</sub>, or arterial blood gas analysis were observed during SPACE or manual insufflation before or after the 20-minute insufflation. However, end-tidal CO<sub>2</sub> and arterial partial pressure of carbon dioxide tended to increase after manual insufflation, and pH tended to decrease.

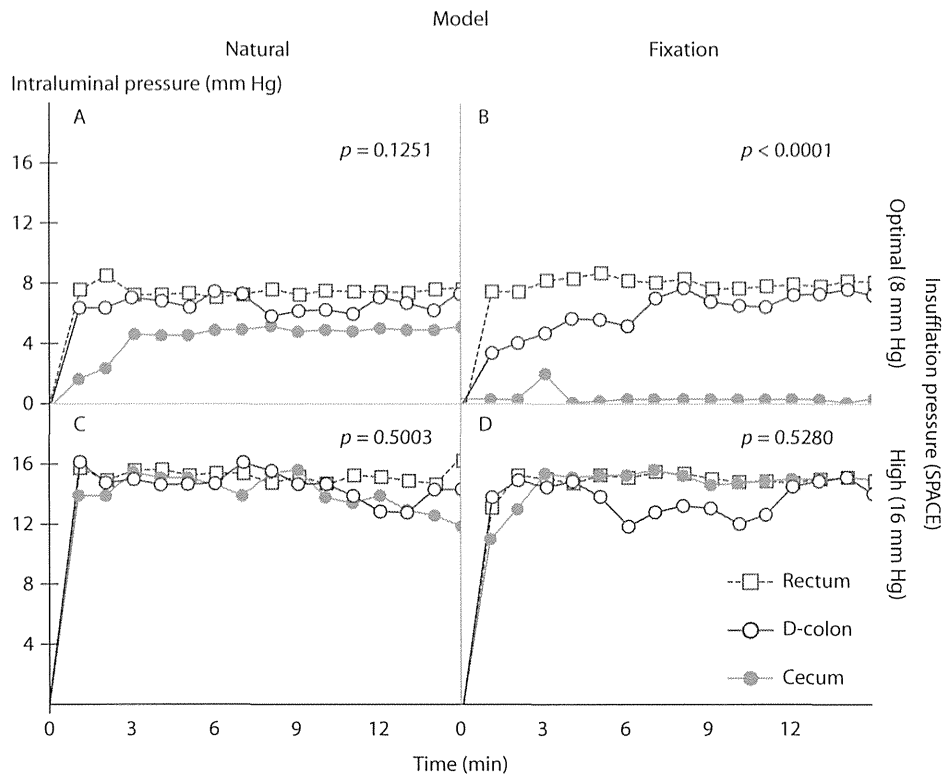


**FIGURE 5.** Changes of intraluminal pressure at each monitoring point during experiment 2. We compared the pressure curves of the distal colon (D-colon) and cecum in each setting to evaluate the pressure difference between the proximal side and the distal side of the colon.

### Experiment 2

The intraluminal pressure changes are shown in Figure 5. With all of the models and pressure settings, the rectal pressure reached the preset value immediately after the commencement of insufflation and remained steady with slight pressure fluctuation (Fig. 5). However, the insufflated gas migrated to the upstream colon (cecum) in natural models with optimal-pressure insufflation (8 mm Hg); the intracecal pressure was  $\approx 5$  mm Hg (Fig. 5A). In contrast, the gas did not migrate to the upstream colon in fixation models with 8-mm Hg insufflation pressure (Fig. 5B). The use of high-pressure insufflation (16 mm Hg) resulted in retrograde gas migration into the cecum with or without artificial fixation of the colon (Figs. 5C and D). Representative x-ray images are shown in Figure 6. In the fixation model, gas migration was not observed in the oral tract beyond the flexure point during optimal-pressure insufflation (Fig. 6B); gas migration was confirmed during high-pressure insufflation (Fig. 6D). In the natural model, gas migration was observed in the oral tract regardless of insufflation pressure (Figs. 6A and C).

### DISCUSSION

Optimal insufflation is the most fundamental and important element to establish adequate endoscopic visualization

and working space.<sup>2,4,17</sup> Our group has engaged in research regarding CO<sub>2</sub> insufflation and the creation of a stable working area in the GI tract.<sup>3,17-20</sup> In a previous trial, esophageal SPACE provided stable visualization with excellent reproducibility, without significant gas migration beyond the duodenum.<sup>4</sup> Thus, we considered SPACE more advantageous than conventional manual insufflation endoscopy because it created stable/comfortable endoscopic exposure and prevented massive gas migration and subsequent prolonged bowel distension. The reduced amount of gas migration in SPACE may be more attractive in the lower GI tract, where migrated gas is known to cause postprocedural abdominal bloating and discomfort.<sup>9,15,21</sup> We examined the feasibility and safety of SPACE colonoscopy to apply SPACE to the lower GI tract.

Experiment 1 confirmed the feasibility of SPACE in the lower GI tract. Our SPACE system created a good and stable endoscopic view in the cecum. We considered 8 mmHg the optimal insufflation pressure for SPACE colonoscopy in the canine cecum; however, we previously reported that 14 mm Hg was suitable for SPACE esophagoscopy in a porcine model. The optimal pressure during SPACE might vary depending on animal species, surgical field, and existing pathology, among other things. We also validated the safety of cecal SPACE: no significant change was noted in any of the cardiopulmonary parameters during the 20-minute cecal SPACE procedure (Table 1).